

Observer design for Lur'e systems via injection of a reconstructed nonlinear output

Adel Malik ANNABI^a

^aINRIA, CNRS, Université Côte d'Azur, France

Abstract

Observer design for Lur'e systems typically reduces to solving a linear matrix inequality (LMI). In certain cases, the observer gain may grow unbounded with the coupling strength. We propose reconstructing key nonlinear terms via a bank of second-order sliding-mode observers and injecting them into a Luenberger observer as additional measurements. This feeds a second correction channel that attenuates the nonlinear coupling in the error dynamics. The convergence of the combined observer is guaranteed under a new LMI which contains the classical one as a special case. We exhibit parameter regimes where classical designs require impractically large gains, while the proposed design maintains moderate gains. A stability analysis of the proposed observer characterizes the trade-off between the two designs and identifies the noise regimes in which the proposed design is preferable. We illustrate the approach on a Wilson–Cowan network showing the trade-off between the nonlinear coupling strength, observer gain, and noise.

Keywords: Observer design; Lur'e systems; LMI; Second-order sliding-mode observers; Sector-bounded nonlinearities; Neural mass models

1. Introduction

Estimating the internal state of a dynamical system from partial measurements is a fundamental problem in control theory. A particularly structured and widely studied class of nonlinear systems is that of Lur'e systems: a linear block in feedback interconnection with a static, memoryless nonlinearity. Lur'e models arise naturally in many application domains, including neuroscience [1, 2, 3, 4], where the state is typically only partially measured and reconstructing the full activity vector is essential for monitoring and closed-loop control.

For Lur'e systems, the standard approach to state estimation is the Luenberger observer, which copies the plant dynamics and corrects the state prediction with a term proportional to the output prediction error. When the nonlinearity satisfies an incremental sector or slope-restricted condition, the convergence of the estimation error can be certified through a

linear matrix inequality (LMI), solvable by semidefinite programming [5, 6, 7, 8, 9]. This LMI-based design has been successfully applied to neural mass models [10, 11] for example.

A known difficulty is that the LMI becomes increasingly stringent as the nonlinear coupling strengthens. When the nonlinear feedback dominates the linear dynamics, the LMI may become infeasible under any reasonable bound on the observer gain. The solver is then forced either to return gains that are too large to be deployed in practice, or to declare infeasibility altogether. In either case, no usable Luenberger observer is produced.

As this obstruction is fundamentally a lack of measurements, the core idea of this work is that if we had access to key nonlinear terms, one could inject them in the Luenberger observer and relax the LMI accordingly. We show that, for the considered class of Lur'e systems, these signals can be reconstructed from the output itself. Defining the auxiliary variables $z_1 = CV$ and $z_2 = CAV + CWS(V)$, the dynamics per output channel take the triangular form $\dot{z}_{1,j} = z_{2,j} + [CBu]_j$. A bank of homogeneous observers [12, 13, 14] recovers z_2 from z_1 in finite

Email addresses: adel-malik.annabi@inria.fr (Adel Malik ANNABI), adel.malik.annabi@proton.me (Adel Malik ANNABI)

time, yielding an additional *virtual measurement* of the nonlinear coupling as seen through the output.

With this virtual measurement, we augment the classical Luenberger observer with a second correction channel that compares the predicted nonlinear output against the reconstructed signal. The convergence of the resulting combined observer is guaranteed by a new LMI that contains the classical one as a special case. Because the second channel attenuates the effective nonlinear coupling before it reaches the error dynamics, the new LMI remains feasible and yields moderate gains in regimes where the classical one either fails or demands gains orders of magnitude larger. However, the approach introduces the cost of the reconstruction of the virtual measurement, which requires a bank of sliding-mode observers and contributes its own sensitivity to measurement noise. In this regard, we provide a stability analysis that quantifies the steady-state error under bounded measurement noise for both the classical and the proposed observer. This analysis delineates the noise regimes in which each design is preferable and shows that the trade-off, that is accepting the sliding-mode observer's noise footprint in exchange for a drastically reduced observer gain, is favourable across a broad range of operating conditions.

The paper is organized as follows. Section 2 states the system class and the sector condition. Section 3 presents the combined observer and the main convergence theorem with its Lyapunov-based proof. Section 4 establishes the feasibility inclusion between the classical and proposed LMIs and proves, on an illustrative rank-one case, that the new LMI is structurally independent of the coupling strength. Section 5 derives the ISS bound under measurement noise. Section 6 provides a numerical comparison on a Wilson–Cowan network, illustrating the gain reduction and the noise trade-off. Section 7 concludes.

2. Problem statement

Consider the Lur'e system

$$\begin{cases} \dot{V} = AV + WS(V) + Bu + p(t), \\ y = CV + n(t), \end{cases} \quad (1)$$

where $V \in \mathbb{R}^n$ is the state, $u \in \mathbb{R}^{n_u}$ the input, $y \in \mathbb{R}^{n_y}$ the measured output, and $p(t)$, $n(t)$ are bounded disturbances with $\|p(t)\| \leq \bar{p}$, $\|n(t)\| \leq \bar{n}$ uniformly in t . The matrices $A \in \mathbb{R}^{n \times n}$, $W \in \mathbb{R}^{n \times n}$, $B \in \mathbb{R}^{n \times n_u}$, $C \in \mathbb{R}^{n_y \times n}$ are known.

The nonlinearity $S : \mathbb{R}^n \rightarrow \mathbb{R}^n$ is assumed to satisfy the following incremental sector condition: there exist diagonal matrices $\Gamma = \text{diag}(\gamma_1, \dots, \gamma_n) \succeq 0$ and $\Lambda = \text{diag}(\lambda_1, \dots, \lambda_n) \succ 0$ such that, for all $x, \hat{x} \in \mathbb{R}^n$, setting $\delta = S(\hat{x}) - S(x)$ and $e = \hat{x} - x$,

$$\sum_{i=1}^n \lambda_i \delta_i (\delta_i - \gamma_i e_i) \leq 0. \quad (2)$$

Two classical conditions that guarantee (2) [6, 7] are recalled below.

- (i) *Component-wise slope bound.* If S acts component-wise and each S_i satisfies $0 \leq S'_i(\xi) \leq \gamma_i$ for all $\xi \in \mathbb{R}$ [7], then (2) holds for any diagonal $\Lambda \succ 0$.
- (ii) *Global operator bound.* If S has a symmetric Jacobian with $0 \preceq J_S(V) \preceq \gamma I$ for all V , the integral mean-value theorem gives $\delta = \bar{J}e$ with $0 \preceq \bar{J} \preceq \gamma I$, so $\delta^\top \lambda (\delta - \gamma e) \leq 0$; (2) holds with $\Gamma = \gamma I$ and scalar $\Lambda = \lambda I$. This condition is satisfied by Galerkin approximations of neural field models [2].

We also consider the weaker case where only component-wise monotonicity $\delta_i e_i \geq 0$ is known (no slope bound γ_i is available); the corresponding increasing-only LMI is derived in Remark 8.

Assumption 1. *Solutions of (1) are bounded in a known compact set $\mathcal{K} \subset \mathbb{R}^n$ for all admissible inputs.*

This assumption is standard in the literature. If, for example, the matrix A is Hurwitz and the nonlinearity S is bounded, then it is verified.

Observer design problem. Construct an auxiliary system driven by (y, u) whose state \hat{V} satisfies $\|\hat{V}(t) - V(t)\| \rightarrow 0$ exponentially for all initial conditions $\hat{V}(0)$ in a given set.

3. Combined observer and convergence theorem

The proposed observer uses both the measured output $y = CV$ and the signal $y_2 := CAV + CWS(V)$, which is reconstructed in finite time from y . The full system is

$$\begin{cases} \dot{\hat{z}}_{1,j} = \hat{z}_{2,j} + [CBu]_j + L_j k_1 [y_j - \hat{z}_{1,j}]^{1/2}, \\ \dot{\hat{z}}_{2,j} \in L_j^2 k_2 \text{sign}(y_j - \hat{z}_{1,j}), \quad j = 1, \dots, n_y, \\ \dot{\hat{V}} = A\hat{V} + WS(\hat{\zeta}) + K(y - C\hat{V}) \\ \quad - K'(CA\hat{V} + CWS(\hat{\zeta}) - \hat{z}_2) + Bu, \end{cases} \quad (3)$$

where $\hat{\zeta} = \hat{V} + E(y - C\hat{V})$, $[\cdot]^{1/2} = |\cdot|^{1/2} \text{sign}(\cdot)$, and $K, K' \in \mathbb{R}^{n \times n_y}$, $E \in \mathbb{R}^{n \times n_y}$, $L_j > 0$, $k_1, k_2 > 0$ are design parameters (the gains k_1, k_2 are standard for the homogeneous observer; see [12]). The matrix E shifts the argument of S inside the sector, reducing conservatism [7]. The coupling attenuation of the present design is achieved via K' and does not rely on E ; we set $E = 0$ in all numerical results, which keeps the matrix inequality linear (Remark 14).

The upper block is a bank of n_y parallel second-order sliding-mode observers (solutions understood in the Filippov sense [12]) that reconstruct $y_2 = CAV + CWS(V)$ from y ; the lower block is the Lur'e-type injection observer that uses both y and the estimate \hat{z}_2 .

3.1. Design steps (heuristics).

1. Defining $z_{1,j} = [CV]_j$ and $z_{2,j} = [CAV + CWS(V)]_j$, the dynamics per channel satisfy $\dot{z}_{1,j} = z_{2,j} + [CBu]_j$, a scalar triangular form [14] with known feedforward $[CBu]_j$. Under Assumption 1, $\hat{z}_{2,j}$ is bounded; a homogeneous observer [12, 13] then recovers $z_{2,j}$ from $z_{1,j}$ in prescribed finite time T_0 for sufficiently large L_j [13, 14]. The observer acts as a robust exact reconstructor and delivers $\hat{z}_2 = z_2$. For $A = -\lambda I$ (Wilson–Cowan; Section 6), we have $z_2 = CWS(V)$ only, reducing the required gain L_j .

2. Once $\hat{z}_2(t) = y_2(t)$ for $t \geq T_0$, the lower observer is driven by both y and the exact y_2 . With $e = \hat{V} - V$, $\hat{\zeta} - V = (I - EC)e$, and $\delta = S(\hat{\zeta}) - S(V)$, the error dynamics become

$$\dot{e} = [(I - K'C)A - KC]e + (I - K'C)W\delta. \quad (4)$$

Gain K' replaces W by $(I - K'C)W$ in the coupling term, while K damps the linear part and E shifts the sector argument.

3. Solve for (K, K', E, P, Λ) to satisfy the LMI (8) (Theorem 5).

The architecture adds $2n_y$ scalar states to the n states of the Lur'e observer; when $n_y \ll n$ this overhead is negligible. The second-order sliding-mode gains L_j must be tuned per channel and the discontinuous right-hand side requires a dedicated integration scheme [13].

Proposition 2 (Homogeneous observer). *Under Assumption 1, consider the homogeneous observer (upper block of (3)), restated per channel $j = 1, \dots, n_y$ as*

$$\dot{\hat{z}}_{1,j} = \hat{z}_{2,j} + [CBu]_j + L_j k_1 [y_j - \hat{z}_{1,j}]^{1/2}, \quad (5)$$

$$\dot{\hat{z}}_{2,j} \in L_j^2 k_2 \text{sign}(y_j - \hat{z}_{1,j}), \quad (6)$$

under the perturbed system (1). There exist constants k_1, k_2 such that, for any $\bar{p}, \bar{n} > 0$, there exist $L_j^* \geq 1$, a class- \mathcal{KL} function β , and constants $\gamma, \mu > 0$ (depending on \bar{p}, \bar{n} and on the system data: $\|W\|, \|C\|$, the Lipschitz constant of S , and \mathcal{K}) such that, for all $L_j \geq L_j^*$, any solution of the combined system (1)–(6) satisfies, for all $t \geq 0$,

$$|\hat{z}_{2,j}(t) - [CAV(t) + CWS(V(t))]_j| \leq \max\left(\beta(|\hat{z}_j(0) - z_j(0)|, t), \gamma(L_j^{1/2} \bar{n}^{1/2} + \bar{p}/L_j^\mu)\right). \quad (7)$$

In the absence of noise and disturbances ($\bar{n} = \bar{p} = 0$), $\hat{z}_{2,j}(t) = [CAV(t) + CWS(V(t))]_j$ for all $t \geq T_0$, for some $T_0 > 0$.

Proof. Define $z_{1,j} = [CV]_j$ and $z_{2,j} = [CAV + CWS(V)]_j$. Differentiating along (1) with disturbance p , $\dot{z}_{1,j} = z_{2,j} + [CBu]_j + [Cp]_j$, $y_{\text{meas},j} = z_{1,j} + n_j$, which is the triangular form [14] with $m = 2$, $\Phi_1 = [CBu]_j$, $w_1 = [Cp]_j$, and $v = n_j$. The second channel is

$$\dot{z}_{2,j} = [C(I + W\partial_V S(V))(AV + WS(V) + p(t) + Bu(t))]_j := \Phi_2(z_{1,j}, z_{2,j}, V(t), t).$$

Under Assumption 1, $V \in \mathcal{K}$, S is Lipschitz, and Φ_2 involves $A, W, C, S(V)$, and the Jacobian of S along the flow; hence Φ_2 is uniformly bounded by a constant depending on $\|W\|, \|C\|$, the Lipschitz constant of S , and \mathcal{K} . Crucially, the expression of Φ_2 need not be known. The observer (5)–(6) is the homogeneous observer of [14] with $d_0 = -1$. The ISS bound (7) follows from [14, Proposition 4] (Eq. (16) for $d_0 = -1$); the disturbance Φ_2 on the second channel does not enter the steady-state estimate. The noiseless convergence is the special case $\bar{n} = \bar{p} = 0$. \square

Remark 3 (Convergence speed versus noise amplification). *The \mathcal{KL} function β in (7) can be made arbitrarily fast by increasing L_j : for any prescribed $T_0 > 0$, there exists L_j large enough such that the \mathcal{KL} transient is dominated by the steady-state term*

for all $t \geq T_0$. For $t \geq T_0$, the reconstruction error then reduces to $|\hat{z}_{2,j} - z_{2,j}| \leq \gamma(L_j^{1/2} \bar{n}^{1/2} + \bar{p}/L_j^\mu)$. Increasing L_j thus reduces the convergence time but amplifies the $L_j^{1/2}$ factor in the noise floor—the fundamental trade-off between speed and noise sensitivity [12, 13, 15, 14].

Remark 4 (Structure of the combined design). *The classical LMI (13) forces a single gain K to simultaneously stabilise the linear error dynamics and absorb the coupling PW , both through the same Lyapunov matrix P . The combined design separates these tasks into three specialised parameters:*

- (i) K' attenuates coupling geometrically, replacing PW by $PP_{\ker C}W$ in the LMI off-diagonal (see Proposition 11 in Section 4);
- (ii) K stabilises the residual linear error dynamics with attenuated coupling;
- (iii) L_j ($j = 1, \dots, n_y$) reconstruct the coupling components visible through the output, each governed by an existential condition: there exists a threshold L_j^* such that exact reconstruction holds for all $L_j \geq L_j^*$ [12, 13, 14].

A single fixed $L_j = 3$ suffices across the full tested range $s \in [0.5, 100]$ in Section 6.

Theorem 5 (Combined observer). *Under Assumption 1, suppose there exist $P \succ 0$, diagonal $\Lambda \succ 0$, $q > 0$, and matrices K, K', E such that*

$$\begin{pmatrix} \text{He}\{PA - PK'CA - PKC\} + qI & P(I - K'C)W + (I - EC)^\top \Gamma^\top \Lambda \\ W^\top (I - K'C)^\top P + \Lambda \Gamma (I - EC) & -2\Lambda \end{pmatrix} \preceq 0. \quad (8)$$

Then, in the noise-free case ($n \equiv 0$, $p \equiv 0$), for any $L_j \geq L_j^*$ ($j = 1, \dots, n_y$), where L_j^* are the thresholds from Proposition 2, the observer (3) achieves $\|e(t)\| \leq Me^{-\rho(t-T_0)}\|e(T_0)\|$ for all $t \geq T_0$, with $M = \sqrt{\lambda_{\max}(P)/\lambda_{\min}(P)}$ and $\rho = q/(2\lambda_{\max}(P))$.

Proof. For $t \geq T_0$, Proposition 2 gives $\hat{z}_2(t) = y_2(t)$ exactly. Thus $e = \hat{V} - V$ satisfies (4) with $\delta = S(\hat{\zeta}) - S(V)$ and $\hat{\zeta} - V = (I - EC)e$. Applying the sector condition (2) with $\hat{x} = \hat{\zeta}$, $x = V$:

$$\sum_{i=1}^n \lambda_i \delta_i (\delta_i - \gamma_i [(I - EC)e]_i) \leq 0. \quad (9)$$

Consider $\mathcal{V}(e) = e^\top P e$. Its derivative along (4) is

$$\dot{\mathcal{V}} = e^\top \text{He}\{P[(I - K'C)A - KC]\}e$$

$$+ 2e^\top P(I - K'C)W\delta.$$

The sector condition (9) gives in matrix form $\delta^\top \Lambda (\delta - \Gamma(I - EC)e) \leq 0$. Following the standard Lyapunov analysis for Lur'e observers [6, 7], adding this nonnegative quantity to $\dot{\mathcal{V}}$ yields a sufficient condition for $\dot{\mathcal{V}} \leq -q\|e\|^2$, namely that the quadratic form in $\xi = (e^\top, \delta^\top)^\top$,

$$\begin{pmatrix} e \\ \delta \end{pmatrix}^\top \mathcal{M} \begin{pmatrix} e \\ \delta \end{pmatrix} \leq 0 \quad \text{for all } (e, \delta),$$

where \mathcal{M} is the matrix in (8). Hence $\dot{\mathcal{V}} \leq -q\|e\|^2$, giving $\mathcal{V}(e(t)) \leq \mathcal{V}(e(T_0))e^{-q/\lambda_{\max}(P)(t-T_0)}$, and the stated bound follows from $\lambda_{\min}(P)\|e\|^2 \leq \mathcal{V} \leq \lambda_{\max}(P)\|e\|^2$. \square

Corollary 6 (Output-linear drift). *Suppose $CA = MC$ for a known matrix $M \in \mathbb{R}^{n_y \times n_y}$. Then $CAV = My$ is directly available from the output; the sliding-mode observer only needs to reconstruct $CWS(V)$. The observer simplifies to*

$$\begin{cases} \dot{\hat{z}}_{1,j} = [M\hat{z}_1]_j + \hat{z}_{2,j} + [CBu]_j + L_j k_1 [y_j - \hat{z}_{1,j}]^{1/2}, \\ \dot{\hat{z}}_{2,j} \in L_j^2 k_2 \text{sign}(y_j - \hat{z}_{1,j}), \quad j = 1, \dots, n_y, \\ \dot{\hat{V}} = A\hat{V} + WS(\hat{\zeta}) + K(y - C\hat{V}) \\ \quad - K'(CWS(\hat{\zeta}) - \hat{z}_2) + Bu, \end{cases} \quad (10)$$

and the error dynamics reduce to $\dot{e} = (A - KC)e + (I - K'C)W\delta$. Theorem 5 holds under the same assumptions with the simplified LMI

$$\begin{pmatrix} \text{He}\{PA - PKC\} + qI & P(I - K'C)W + (I - EC)^\top \Gamma^\top \Lambda \\ W^\top (I - K'C)^\top P + \Lambda \Gamma (I - EC) & -2\Lambda \end{pmatrix} \preceq 0. \quad (11)$$

The only difference from (8) is the absence of the $-PK'CA$ term in the (1, 1) block, because CAV is known. The Wilson–Cowan case $A = -\lambda I_n$ corresponds to $M = -\lambda I_{n_y}$.

Proposition 7 (Direct nonlinear output). *Suppose S acts component-wise and each row of C is proportional to a standard basis vector of \mathbb{R}^n (each output channel measures exactly one state component). Then $CS(V) = S(CV) = S(y)$, and consequently $CWS(V) = WS(y)$ is directly computable from the measured output. Corollary 6 applies without Proposition 2; the sliding-mode bank and its associated tuning are eliminated entirely.*

Remark 8 (Increasing-only LMI). *When the nonlinearity is only known to be component-wise increasing ($\delta_i e_i \geq 0$) but no slope bound γ_i is available, the sector condition (2) does not apply and the*

LMI (8) cannot be used. Applying the S -procedure with the increasing condition $\delta^\top \Lambda (I - EC)e \geq 0$ ($\Lambda = \text{diag}(\lambda_i) \succ 0$) to the Lyapunov derivative \dot{V} yields the quadratic form

$$\begin{pmatrix} \text{He}\{P[(I - K'C)A - KC]\} + qI & P(I - K'C)W + (I - EC)^\top \Lambda \\ W^\top (I - K'C)^\top P + \Lambda(I - EC) & 0 \end{pmatrix},$$

whose (2, 2) block vanishes. For this matrix to be negative semidefinite, the off-diagonal must be zero—a condition that is rarely feasible ($PW + (I - EC)^\top \Lambda = 0$ for the classical observer). Adding a small regularisation $-\varepsilon I$ ($\varepsilon > 0$) in the (2, 2) block yields the relaxed LMI

$$\begin{pmatrix} \text{He}\{P[(I - K'C)A - KC]\} + qI & P(I - K'C)W + (I - EC)^\top \Lambda \\ W^\top (I - K'C)^\top P + \Lambda(I - EC) & -\varepsilon I \end{pmatrix} \preceq 0. \quad (12)$$

Compared with (8), the term $(I - EC)^\top \Gamma^\top \Lambda$ in the (1, 2) block is replaced by $(I - EC)^\top \Lambda$ and the damping term -2Λ by $-\varepsilon I$. The combined observer retains its coupling attenuation because K' replaces W by $(I - K'C)W$ in the off-diagonal independently of Γ (and independently of E).

Although it is not obvious that the sliding-mode observer can be used when $\partial_V S$ is unbounded (finite-time convergence proofs typically require boundedness of $\partial_V S$), the numerical simulations show a case where it nonetheless succeeds. This leads to a significant performance gain for the proposed observer design.

Remark 9. On $[0, T_0)$, the sliding-mode observer error $\varepsilon_2(t)$ is bounded by construction [13, 14], and the observer error dynamics $\dot{e} = A_{c1}e + (I - K'C)W\delta + K'\varepsilon_2(t)$, with $A_{c1} = (I - K'C)A - KC$, are locally Lipschitz in e (with ε_2 acting as a bounded exogenous input); hence $e(T_0)$ is finite. The exponential bound of Theorem 5 therefore starts from a bounded initial condition.

4. Comparison with the standard Lur'e LMI

The standard Lur'e LMI [6, 7, 8, 9] (recovered by setting $K' = 0$ in (8)) reads

$$\begin{pmatrix} \text{He}\{PA - PKC\} + qI & PW + (I - EC)^\top \Gamma^\top \Lambda \\ W^\top P + \Lambda \Gamma (I - EC) & -2\Lambda \end{pmatrix} \preceq 0. \quad (13)$$

The coupling matrix W appears in the off-diagonal block of (13) without any design freedom; feasibility requires P and Λ to jointly absorb $\|W\|$. In contrast, (8) replaces W by $(I - K'C)W$ in the off-diagonal block: choosing K' to reduce the effective norm

$\|(I - K'C)W\|$ can lower the observer gains needed to certify a given convergence rate, which is especially useful when the classical design is formally feasible but its gains become very large in practice.

Proposition 10 (Inclusion of feasibility sets). *Any (P, Λ, K, E) feasible for (13) is feasible for (8) with $K' = 0$. Hence the feasibility set of (8) contains that of (13).*

Proposition 11 (Fixed K' choice for coupling reduction). *Assume C has full row rank. For arbitrary A, W, Γ , the choice $K' = C^\top (CC^\top)^{-1}$ yields the effective coupling*

$$\begin{aligned} (I - K'C)W &= P_{\ker C} W, \\ P_{\ker C} &= I - C^\top (CC^\top)^{-1} C, \end{aligned} \quad (14)$$

where $P_{\ker C}$ is the orthogonal projection onto $\ker C$. Consequently the coupling matrix appearing in the off-diagonal term of (8) satisfies $\|(I - K'C)W\| = \|P_{\ker C} W\| \leq \|W\|$, with equality iff $CW = 0$ and strict inequality whenever $CW \neq 0$.

If, in addition, the columns of W lie in $\text{range}(C^\top)$, i.e. $W = C^\top X$ for some X , then $(I - K'C)W = 0$: the nonlinear coupling is completely eliminated from the error dynamics, and the combined LMI (8) reduces to a linear stability condition independent of W . Under the further condition $CA = MC$ (Corollary 6), the simplified LMI (11) applies. If A is Hurwitz, that LMI is then feasible with $K = 0$: the error dynamics are $\dot{e} = Ae$, and the sector condition is absorbed by a free choice of Λ .

Proof. With $K' = C^\top (CC^\top)^{-1}$, $(I - K'C)W = (I - C^\top (CC^\top)^{-1} C)W = P_{\ker C} W$. Since $P_{\ker C}$ is an orthogonal projection, $\|P_{\ker C} W\| \leq \|W\|$, with equality iff $CW = 0$. When $W = C^\top X$, $(I - K'C)W = P_{\ker C} C^\top X = 0$, so the off-diagonal term of (11) reduces to $(I - EC)^\top \Gamma^\top \Lambda$. With $K = 0$, the (1, 1) block is $\text{He}\{PA\} + qI$. Since A is Hurwitz, $P \succ 0$ can be chosen to satisfy $\text{He}\{PA\} = -Q \prec 0$ for any $Q \succ 0$; picking q small enough yields a negative-definite (1, 1) block. Feasibility of the full LMI then follows by the Schur complement with Λ free. \square

Remark 12 (Trade-off in the choice of K'). *While $K' = C^\top (CC^\top)^{-1}$ eliminates the coupling components in the row space of C , the combined LMI (8) also involves K' in the (1, 1) block through $PK'CA$. Choosing K' solely to cancel the coupling may destabilise the linear part $(I - K'C)A$ if A has unstable*

modes in the output directions. In the case $A = -\lambda I$, this trade-off disappears because A and $K'CA$ commute and both contribute damping. More generally, the LMI (8) jointly optimises over (K, K', P, Λ) and automatically balances coupling attenuation against linear stability. The closed-form K' of Proposition 11 serves as an admissible choice with a guaranteed coupling reduction, not necessarily as the LMI-optimal K' .

5. Stability under noise and model disturbances

In practice the output y is corrupted by measurement noise and the model may be subject to a bounded disturbance. The following result quantifies how both perturbations propagate to the observer error, and how the combined observer's smaller effective gain reduces the noise floor relative to the classical design.

Under the perturbed system (1), the per-channel evolution is $\dot{z}_{1,j} = z_{2,j} + [CBu]_j + [Cp]_j$, $y_{\text{meas},j} = z_{1,j} + n_j$. Proposition 2 applies; choosing L_j sufficiently large such that the \mathcal{KL} transient is below the steady-state floor for $t \geq T_0$, the ISS bound (7) reduces to the component-wise estimate

$$\begin{aligned} \hat{z}_{2,j}(t) &= z_{2,j}(t) + \varepsilon_{2,j}(t), \\ |\varepsilon_{2,j}(t)| &\leq c_0 \bar{n}^{1/2} + c_1 \bar{p}, \\ c_0 &= O(\sqrt{L_j}), \quad c_1 = O(1/L_j^\mu), \end{aligned} \quad (15)$$

for $j = 1, \dots, n_y$, where $c_0 \bar{n}^{1/2}$ is the measurement noise contribution and $c_1 \bar{p}$ is the propagation of the disturbance $[Cp]_j$ through the observer [12, 13, 14]. The component-wise bounds imply $\|\varepsilon_2\| \leq \sqrt{\bar{n}_y} (c_0 \bar{n}^{1/2} + c_1 \bar{p}) := \bar{\varepsilon}_2$.

Proposition 13 (Stability under noise and model disturbances). *Suppose the LMI (8) is feasible with $E = 0$ and rate $q > 0$, and \hat{z}_2 satisfies (15) for $t \geq T_0$. Define $\bar{\varepsilon}_2 = \sqrt{\bar{n}_y} (c_0 \bar{n}^{1/2} + c_1 \bar{p})$. Then the error $e(t) = \hat{V}(t) - V(t)$ satisfies, for $t \geq T_0$,*

$$\begin{aligned} \|e(t)\| &\leq M \left(e^{-\rho(t-T_0)} \|e(T_0)\| + \right. \\ &\quad \left. \frac{1}{\rho} (\|K\| \bar{n} + \|K'\| \bar{\varepsilon}_2 + \bar{p}) \right), \end{aligned} \quad (16)$$

where $M = \sqrt{\lambda_{\max}(P)/\lambda_{\min}(P)}$ is the condition number of P and $\rho = q/(2\lambda_{\max}(P))$. For the classical observer ($K' = 0$), the bound reduces to $M(e^{-\rho t} \|e(0)\| + \frac{1}{\rho} (\|K\|_{\text{std}} \bar{n} + \bar{p}))$.

Proof. For $t \geq T_0$, the measurement is $y_{\text{meas}} = CV + n$ with $\|n\| \leq \bar{n}$, and (15) gives $\hat{z}_2 = z_2 + \varepsilon_2$ with $\|\varepsilon_2\| \leq \bar{\varepsilon}_2$. With $E = 0$, we have $\hat{\zeta} = \hat{V}$, hence $\delta = S(\hat{V}) - S(V)$. Substituting y_{meas} and \hat{z}_2 into the observer (3), the process disturbance p enters \dot{e} as $-p$ (from the plant dynamics), and the reconstruction error ε_2 enters through the correction term $-K'(CA\hat{V} + CWS(\hat{V}) - \hat{z}_2) = -K'(CAe + CW\delta - \varepsilon_2)$, contributing $+K'\varepsilon_2$. The full error dynamics are

$$\begin{aligned} \dot{e} &= \underbrace{[(I - K'C)A - KC]}_{:=A_{cl}} e \\ &\quad + (I - K'C)W\delta + Kn(t) + K'\varepsilon_2(t) - p(t). \end{aligned}$$

Define the P -norm $\|e\|_P = \sqrt{e^\top P e}$. Differentiating $\|e\|_P^2 = e^\top P e$ along \dot{e} ,

$$\begin{aligned} \frac{d}{dt} \|e\|_P^2 &= e^\top \text{He}\{PA_{cl}\} e + 2e^\top P(I - K'C)W\delta \\ &\quad + 2e^\top P(Kn + K'\varepsilon_2 - p). \end{aligned}$$

The LMI (8) (with $E = 0$) absorbs the δ terms exactly as in the proof of Theorem 5, giving $e^\top \text{He}\{PA_{cl}\} e + 2e^\top P(I - K'C)W\delta \leq -q\|e\|^2$. Hence

$$\frac{d}{dt} \|e\|_P^2 \leq -q\|e\|^2 + 2e^\top P(Kn + K'\varepsilon_2 - p). \quad (17)$$

Writing $e^\top PKn = (P^{1/2}e)^\top P^{1/2}Kn$ and applying Cauchy–Schwarz,

$$\begin{aligned} e^\top P(Kn + K'\varepsilon_2 - p) &\leq \|e\|_P (\|P^{1/2}K\| \bar{n} + \\ &\quad \|P^{1/2}K'\| \bar{\varepsilon}_2 + \|P^{1/2}\| \bar{p}). \end{aligned}$$

Also $\|e\|_P^2 \leq \lambda_{\max}(P)\|e\|^2$, so $-q\|e\|^2 \leq -\frac{q}{\lambda_{\max}(P)}\|e\|_P^2$. Putting these together,

$$\begin{aligned} \frac{d}{dt} \|e\|_P^2 &\leq -\frac{q}{\lambda_{\max}(P)} \|e\|_P^2 \\ &\quad + 2\|e\|_P (\|P^{1/2}K\| \bar{n} + \|P^{1/2}K'\| \bar{\varepsilon}_2 + \|P^{1/2}\| \bar{p}). \end{aligned}$$

Dividing by $2\|e\|_P$,

$$\begin{aligned} \|\dot{e}\|_P &\leq -\underbrace{\frac{q}{2\lambda_{\max}(P)}}_{\rho} \|e\|_P \\ &\quad + \|P^{1/2}K\| \bar{n} + \|P^{1/2}K'\| \bar{\varepsilon}_2 + \|P^{1/2}\| \bar{p}. \end{aligned}$$

This is a linear differential inequality in $\|e\|_P$. By the comparison lemma [16],

$$\begin{aligned} \|e\|_P(t) &\leq \|e\|_P(T_0)e^{-\rho(t-T_0)} \\ &+ \frac{1}{\rho} (\|P^{1/2}K\|\bar{n} + \|P^{1/2}K'\|\bar{\varepsilon}_2 + \|P^{1/2}\|\bar{p}). \end{aligned}$$

Converting back to the Euclidean norm via $\sqrt{\lambda_{\min}(P)}\|e\| \leq \|e\|_P \leq \sqrt{\lambda_{\max}(P)}\|e\|$ and bounding $\|P^{1/2}\| = \sqrt{\lambda_{\max}(P)}$, $\|P^{1/2}X\| \leq \sqrt{\lambda_{\max}(P)}\|X\|$ for each gain matrix gives $M = \sqrt{\lambda_{\max}(P)/\lambda_{\min}(P)}$ in (16). \square

Remark 14 (Why $E = 0$ in the analysis above and in simulations). *When $E = 0$, the LMI (8) is linear in the decision variables (P, PK, PK', Λ) and can be solved by standard semidefinite programming. With $E \neq 0$, the product $E\Lambda$ makes the condition bilinear, requiring iterative methods [7]. Since the coupling attenuation via K' does not rely on E (Proposition 11), we set $E = 0$ in the stability analysis and in all numerical simulations (Section 6).*

Remark 15 (Noise floor comparison and crossover). *At steady state (16) gives*

$$\begin{aligned} \|e\|_{\text{ss}}^{\text{comb}} &\lesssim \\ \frac{M}{\rho} (\|K\|_{\text{comb}}\bar{n} + \|K'\| (c_0\sqrt{\bar{n}_y}\bar{n}^{1/2} + c_1\sqrt{\bar{n}_y}\bar{p}) + \bar{p}) \end{aligned} \quad (18)$$

and $\|e\|_{\text{ss}}^{\text{std}} \lesssim \frac{M}{\rho} (\|K\|_{\text{std}}\bar{n} + \bar{p})$. *The combined observer benefits from $\|K\|_{\text{comb}} \ll \|K\|_{\text{std}}$ but pays a $\bar{n}^{1/2}$ -scaling penalty through the sliding-mode observer noise $c_0\sqrt{\bar{n}_y}\bar{n}^{1/2}$. For $\bar{p} = 0$, the crossover noise level below which the classical observer outperforms satisfies $\bar{n}_{\text{cross}} \approx (\|K'\|\sqrt{\bar{n}_y}c_0/\|K\|_{\text{std}})^2$, with the numerically observed crossover at $\sigma \approx 2 \cdot 10^{-2}$ (Figure 5).*

6. Numerical simulations

6.1. Model and simulation setup

We consider a generalized Wilson–Cowan model [1, 17] with $n_b = 3$ excitatory and 3 inhibitory nodes ($n = 6$). Grouping the excitatory states $V_e \in \mathbb{R}^{n_b}$ and inhibitory states $V_i \in \mathbb{R}^{n_b}$ into $V = (V_e^\top, V_i^\top)^\top$, the dynamics read

$$\begin{cases} \dot{V}_e = A_{ee}V_e + A_{ei}V_i + W_{ee}S(V_e) + W_{ei}S(V_i), \\ \dot{V}_i = A_{ie}V_e + A_{ii}V_i + W_{ie}S(V_e) + W_{ii}S(V_i), \\ y = CV, \end{cases} \quad (19)$$

with block connectivity matrix

$$W = \begin{pmatrix} W_{ee} & W_{ei} \\ W_{ie} & W_{ii} \end{pmatrix}, \quad W_s = sW, \quad s > 0, \quad (20)$$

where s scales the overall coupling strength. Unless stated otherwise, the measurement matrix $C \in \mathbb{R}^{n_y \times n}$ is such that each output channel is a linear combination of two state components, one from the V_e block and one from the V_i block ($n_y = n_b = 3$). All simulations use $n = 6$, $n_y = 3$, a baseline coupling $\|W_0\| = 4.4$, and sliding-mode observer gains $L_j = 3$ ($j = 1, 2, 3$) with $k_1 = 1.5$, $k_2 = 1.1$ in (5)–(6). The plant and observers are integrated with RK4 at $\Delta t = 10^{-3}$ s for 10 s. Zero-mean Gaussian noise of standard deviation σ corrupts y ; process noise of the same level is added to the plant. The root-mean-square (RMS) estimation error

$$\|e\|_{\text{rms}} = \left(\frac{1}{4} \int_6^{10} \|e(t)\|^2 dt \right)^{1/2}$$

is computed over the last 40% of each trajectory.

We present three cases of increasing complexity, each highlighting a different facet of the combined design.

6.2. Case 1: Direct output, no sliding-mode reconstruction

We first illustrate the simplest scenario: Proposition 7, where each output channel measures exactly one state component ($C = [I_3 \ 0_{3 \times 3}]$). Then $CS(V) = S(CV) = S(y)$ is directly available from the output, and the sliding-mode bank is unnecessary (Proposition 7). The observer (3) reduces to

$$\dot{\hat{V}} = A\hat{V} + WS(\hat{V}) + K(y - C\hat{V}) - K'(CS(\hat{V}) - S(y)), \quad (21)$$

with A a general Hurwitz matrix ($\max \Re \lambda(A) = -0.77$). The error dynamics are $\dot{e} = (A - KC)e + (W - K'C)\delta$.

To demonstrate that the coupling attenuation via K' does not rely on a slope bound, we use the Hölder nonlinearity $S(\xi) = |\xi|^{1/2} \text{sign}(\xi)/(1 + |\xi|^{1/2})$, which is bounded, strictly increasing, and satisfies $S'(0) = +\infty$ i.e. no global sector bound exists. The observer gains are computed with the increasing-only LMI (no Γ), see 8.

Table 1 reports the gain norms. The classical increasing-only LMI becomes infeasible at $s \geq 10$, while the combined LMI remains feasible with moderate gains across the full range.

Table 1: Case 1 — Direct output, Hölder S , increasing-only LMI. Classical LMI infeasible for $s \geq 10$; combined LMI remains feasible.

s	$\ W_s\ $	$\ K\ _{\text{std}}$	$\ K\ _{\text{comb}}$	$\ K'\ $
0.5	2.2	7778	54.4	18.1
1.0	4.4	1925	36.3	15.6
5.0	22.0	1943	37.5	32.1
10.0	44.0	—	43.3	56.0
15.0	66.0	—	52.7	80.6
50.0	220.0	—	176.5	268.7

Figure 1 shows the noise sweep at $s = 10$; the combined observer tracks the state accurately despite the absence of any slope bound, achieving RMS ≈ 0.18 at $\sigma = 1$.

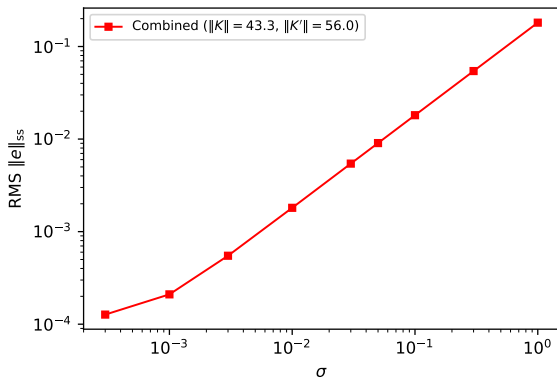


Figure 1: Case 1 — Noise sweep at $s = 10$ ($\|W\| = 44.0$). No sliding-mode bank; $CS(V) = S(y)$ directly. The Classical LMI is infeasible; the combined observer converges.

6.3. Case 2: Hölder nonlinearity with sliding-mode bank

We now consider the LFP-type measurement matrix introduced above, for which $CS(V)$ is not directly available from y . The sliding-mode bank of Proposition 2 reconstructs $CWS(V)$ (the WC form with $A = -\lambda I$). The nonlinearity is the same Hölder function as in Case 1, so no sector bound exists and only the increasing-only LMI applies.

Remark 16 (Sliding-mode observer for $S(0) = 0$, $\alpha \geq 1/2$). When $S(0) = 0$ and S is component-wise Hölder with exponent $\alpha \geq 1/2$, the product $S'(V_i)\dot{V}_i$ remains bounded along trajectories of the Hurwitz system $\dot{V} = -\lambda V + WS(V)$. Near the origin, $\dot{V} = O(\|V\|^\alpha)$ while $S'(V) = O(\|V\|^{\alpha-1})$, so

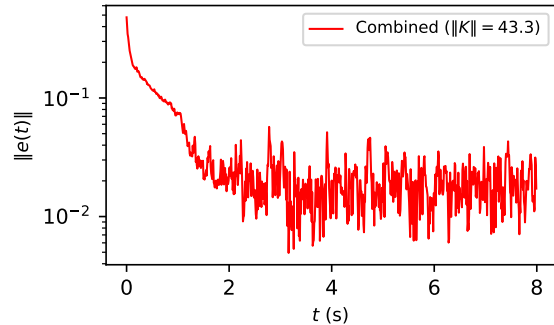


Figure 2: Case 1: Estimation error $\|e(t)\|$ at $s = 10$, $\sigma = 0.1$. Classical LMI infeasible; combined observer converges.

$S'(V_i)\dot{V}_i = O(\|V\|^{2\alpha-1})$, which is $O(1)$ for $\alpha \geq 1/2$. Proposition 2 therefore applies.

Table 2 reports the gain norms. The classical observer requires gains that grow from 1763 to 30701, while the combined observer maintains $\|K\|_{\text{comb}}$ below 30 and $\|K'\|$ stays constant at 2.3—the coupling attenuation is purely geometric.

Table 2: Case 2 — Hölder S + sliding-mode bank, increasing-only LMI. $\|K'\|$ constant; $\|K\|_{\text{std}}$ explodes.

s	$\ W_s\ $	$\ K\ _{\text{std}}$	$\ K\ _{\text{comb}}$	$\ K'\ $
0.5	2.2	1763	6.3	2.3
1.0	4.4	1889	4.0	2.3
5.0	22.0	2178	8.2	2.3
10.0	44.0	3277	10.5	2.3
20.0	88.0	5368	21.5	2.3
50.0	220.0	30701	29.1	2.3

Figure 3 shows the noise sweep at $s = 10$. At very low noise ($\sigma \lesssim 3 \cdot 10^{-4}$), the sliding-mode bank error dominates and the classical observer has a slightly lower error floor. Above $\sigma \approx 3 \cdot 10^{-3}$, the classical gain explosion overtakes the sliding-mode penalty: the combined observer achieves a $13\times$ lower RMS error at $\sigma = 1$. This crossover is consistent with the ISS analysis of Proposition 13: although the sliding-mode term $\propto \sigma^{1/2}$ always dominates the linear term $\propto \sigma$ for $\sigma < 1$, its coefficient $\|K'\|\sqrt{L_j} \approx 4$ is much smaller than $\|K\|_{\text{std}} = 219$, so the classical gain amplification overtakes the sliding-mode penalty once $\sigma \gtrsim (\|K'\|\sqrt{L_j}/\|K\|_{\text{std}})^2$.

6.4. Case 3: Sigmoid with sliding-mode bank

We return to the original Wilson–Cowan configuration with the sigmoid nonlinearity $S(\xi) = 1/(1 +$

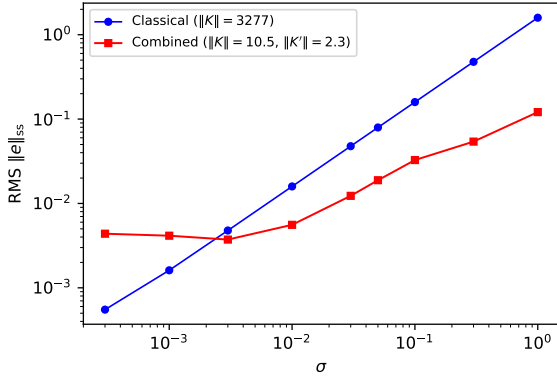


Figure 3: Case 2 — Noise sweep at $s = 10$ ($\|W\| = 44.0$). Sliding-mode bank reconstructs $CWS(V)$. Ratio reaches $13\times$ at $\sigma = 1$.

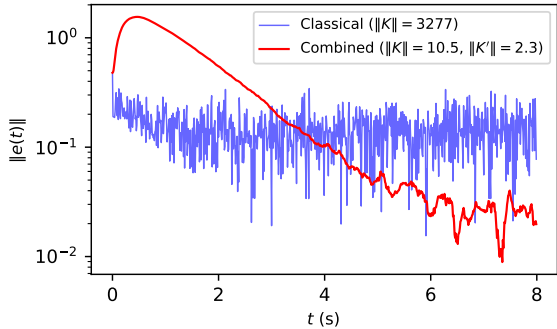


Figure 4: Case 2: Estimation error $\|e(t)\|$ at $s = 10$, $\sigma = 0.1$. Combined observer ($\|K\|_{\text{comb}} = 10.5$) vs. classical ($\|K\|_{\text{std}} = 3277$). The sliding-mode bank converges within $t \in [0, 1]$, producing a transient overshoot; thereafter the combined observer settles at a lower error floor.

$e^{-\lambda_{\text{sig}}\xi}$), $\lambda_{\text{sig}} = 4$, and the LFP measurement matrix C . The tight sector bound $\Gamma = (\lambda_{\text{sig}}/4)I_6 = I_6$ is used in the LMI. The sliding-mode bank reconstructs $CWS(V)$ as in Case 2.

Table 3 reports the gain norms. Both designs attain the maximum convergence rate $q = 10.00$. $\|K\|_{\text{std}}$ grows from 19 to 1271, while $\|K\|_{\text{comb}}$ grows from 5.7 to 50 and $\|K'\|$ stays in $[2.3, 3.1]$.

Figure 5 shows the noise sweep at $s = 15$. Below $\sigma \approx 2 \cdot 10^{-2}$ the sliding-mode observer error $\|K'\|\bar{\varepsilon}_2$ dominates and the classical observer has a lower error floor. Above this crossover, the $\|K\|_{\text{std}}\sigma$ term overtakes the sliding-mode penalty: the $13\times$ smaller gain of the combined observer translates into a $3.8\times$ lower RMS error at $\sigma = 1$. This crossover is predicted by the ISS bound: while the

Table 3: Case 3 — Lipschitz sigmoid + sliding-mode bank, sector LMI. $\|K'\|$ nearly constant; $\|K\|_{\text{std}}$ grows $65\times$.

s	$\ W_s\ $	$\ K\ _{\text{std}}$	$\ K\ _{\text{comb}}$	$\ K'\ $
0.5	2.2	19	5.7	3.1
1.0	4.4	31	6.1	2.7
5.0	22.0	95	10.4	2.4
10.0	44.0	156	13.6	2.4
20.0	88.0	283	19.5	2.3
50.0	220.0	666	33.3	2.3
100.0	440.0	1271	49.9	2.3

$\sigma^{1/2}$ sliding-mode term dominates at low σ , its coefficient $\|K'\|\sqrt{L_j} \approx 4$ is dwarfed by $\|K\|_{\text{std}} = 219$, so the classical observer's linear noise amplification overtakes it.

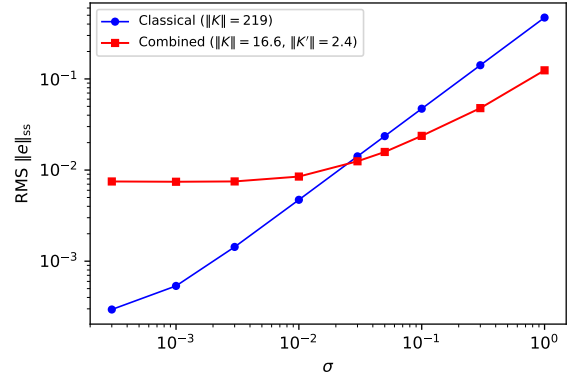


Figure 5: Case 3 — Noise sweep at $s = 15$ ($\|W\| = 66.0$). Crossover near $\sigma \approx 2 \cdot 10^{-2}$; ratio $3.8\times$ at $\sigma = 1$.

7. Conclusion

We have proposed a combined observer for Lur'e systems with a general sector-bounded nonlinearity that augments the standard linear output injection with a nonlinear injection based on the finite-time reconstructed signal $y_2 = CAV + CWS(V)$. The key contributions are:

- (i) an LMI (8) that contains the classical one as a special case and reshapes the coupling term via K' , so the observer gains remain moderate at prescribed convergence rates even when the classical design becomes gain-explosive (Theorem 5, Proposition 11);
- (ii) an increasing-only LMI (Remark 8) that does not require a sector slope bound and remains

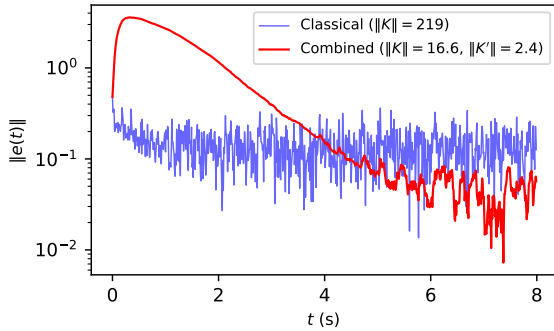


Figure 6: Case 3: Estimation error $\|e(t)\|$ at $s = 15$, $\sigma = 0.3$ (above the crossover). Combined observer ($\|K\|_{\text{comb}} = 16.6$) vs. classical ($\|K\|_{\text{std}} = 219$). As in Case 2, the sliding-mode bank convergence produces a transient overshoot; the combined observer then settles at a lower steady-state error.

feasible for the combined observer when the classical LMI becomes infeasible;

- (iii) structural conditions under which the sliding-mode bank simplifies : $CA = MC$ (Corollary 6) and direct availability of $CS(V)$ from y (Proposition 7);
- (iv) a stability analysis (Proposition 13) quantifying how the combined observer's linear-noise amplification scales with the moderate $\|K\|_{\text{comb}}$ rather than the coupling-dependent $\|K\|_{\text{std}}$, at the cost of an additional error from the sliding-mode observer, with a characterisation of the noise crossover below which the classical design may be preferable;
- (v) numerical confirmation across three scenarios of increasing complexity: (i) direct output without sliding-mode bank, where the classical increasing-only LMI becomes infeasible at moderate coupling while the combined observer remains feasible (Section 6.2); (ii) a Hölder nonlinearity with sliding-mode reconstruction, where $\|K'\|$ stays constant (2.3) and the combined observer achieves a $13\times$ lower RMS error at $\sigma = 1$ (Section 6.3); (iii) the Lipschitz sigmoid model, where the noise crossover is quantified and the combined observer achieves $3.8\times$ lower error (Section 6.4).

References

- [1] H. Wilson, J. Cowan, Excitatory and inhibitory interactions in localized populations of model neurons, *Biophysical Journal* 12 (1) (1972) 1–24.
- [2] S. Amari, Dynamics of pattern formation in lateral-inhibition type neural fields, *Biological Cybernetics* 27 (1977) 77–87.
- [3] B. Jansen, V. Rit, Electroencephalogram and visual evoked potential generation in a mathematical model of coupled cortical columns, *Biological Cybernetics* 73 (4) (1995) 357–366.
- [4] M. Breakspear, Dynamic models of large-scale brain activity, *Nature Neuroscience* 20 (3) (2017) 340–352.
- [5] S. Boyd, L. El Ghaoui, E. Feron, V. Balakrishnan, *Linear Matrix Inequalities in System and Control Theory*, SIAM, 1994.
- [6] M. Arcak, P. Kokotovic, Nonlinear observers: a circle criterion design and robustness analysis, *Automatica* 37 (12) (2001) 1923–1930.
- [7] X. Fan, M. Arcak, Observer design for systems with multivariable monotone nonlinearities, *Systems & Control Letters* 50 (4) (2003) 319–330.
- [8] A. Zemouche, M. Boutayeb, On LMI conditions to design observers for Lipschitz nonlinear systems, *Automatica* 49 (2) (2013) 585–591.
- [9] M. Giaccagli, V. Andrieu, S. Tarbouriech, D. Astolfi, LMI conditions for contraction, integral action, and output feedback stabilization for a class of nonlinear systems, *Automatica* 154 (2023) 111106.
- [10] M. Chong, R. Postoyan, D. Nešić, L. Kuhlmann, A. Varsavsky, A robust circle criterion observer with application to neural mass models, *Automatica* 48 (11) (2012) 2986–2989.
- [11] C. Liu, X. Zhan, S. Tan, L. Kuhlmann, A. Varsavsky, Robust observer design for neural mass models, *Systems & Control Letters* 63 (2014) 12–19.
- [12] A. Levant, Higher-order sliding modes, differentiation and output-feedback control, *International Journal of Control* 76 (9–10) (2003) 924–941.

- [13] J. Moreno, M. Osorio, A Lyapunov approach to second-order sliding mode controllers and observers, in: Proc. IEEE Conf. Decision and Control, 2008, pp. 2856–2861.
- [14] P. Bernard, L. Praly, V. Andrieu, Observers for a non-lipschitz triangular form, *Automatica* 82 (2017) 301–313.
- [15] J. Moreno, M. Osorio, Strict Lyapunov functions for the super-twisting algorithm, *IEEE Transactions on Automatic Control* 57 (4) (2012) 1035–1040.
- [16] H. Khalil, *Nonlinear Systems*, 3rd Edition, Prentice Hall, 2002.
- [17] H. Wilson, J. Cowan, A mathematical theory of the functional dynamics of cortical and thalamic nervous tissue, *Kybernetik* 13 (2) (1973) 55–80.